REPORT DOCUMENTATION PAGE

Form Approved
OMB No. 0704-0188

1. REPORT DATE *(DD-MM-YYYY)*	**2. TYPE REPORT**	**3. DATES COVERED** *(From - To)*
20-08-2007	JOURNAL ARTICLE	01 Jul 07

4. TITLE AND SUBTITLE

Indirect Dominant Mode Rejection: A Solution to Low Sample Support Beamforming

5a. CONTRACT NUMBER

5b. GRANT NUMBER

5c. PROGRAM ELEMENT NUMBER
61102F

6. AUTHOR(S)

*Ernesto L. Santos, *Michael D. Zoltowski, Muralidhar Rangaswamy

5d. PROJECT NUMBER
2311

5e. TASK NUMBER
HE

5f. WORK UNIT NUMBER
02

7. PERFORMING ORGANIZATION NAME(S) AND ADDRESS(ES)

AFRL/SNHE
80 Scott Drive
Hanscom AFB MA 01731

*Purdue University
School of Electrical And Computer Engineering
West Lafayette IN 47907

8. PERFORMING ORGANIZATION REPORT

9. SPONSORING / MONITORING AGENCY NAME(S) AND ADDRESS(ES)

Electromagnetics Technology Division SC: 437490
Sensors Directorate
Air Force Research Laboratory
80 Scott Drive
Hanscom AFB MA 01731-2909

10. SPONSOR/MONITOR'S ACRONYM(S)

AFRL-SN-HS

11. SPONSOR/MONITOR'S REPORT NUMBER(S)

AFRL-SN-HS-TP-2007-0006

12. DISTRIBUTION / AVAILABILITY STATEMENT

Approved for public release; distribution unlimited.

13. SUPPLEMENTARY NOTES

Published in IEEE Transactions on Signal Processing, Vol. 55, No, 7 July 2007.
Cleared for public release by ESC/PA: ESC-06-0587 dtd 19 May 06

14. ABSTRACT

The work developed and described in this technical report deals with the problem of providing a statistical model of the backscattering from lake surface for low-grazing angle and high resolution radar systems. First described is a statistical analysis of the amplitude of the high-resolution polarimetric data characterized by different radar looking directions with respect to the wind blowing directions. Then, based on the electromagnetic two-scale model, analyzed were both the amplitude and frequency modulations induced on the small-scale Bragg resonant waves by the large-scale surface tilt and advection, due to the swell presence. Our results confirm the lake clutter non-stationarity already found in previous analysis of other sea and lake clutter data. Moreover, the relationship between the variation of clutter spectral features, like texture, Doppler centroid and bandwidth, have been investigated by processing real recorded data. The data used for the research activity have been recorded by the IPIX radar of McMaster University in Grimsby, Ontario, Canada in 1998.

15. SUBJECT TERMS

Statistical analysis lake surface scattering, high-resolution polarimetric data characterization, small-scale Bragg resonant waves, lake clutter non-stationarity

16. SECURITY CLASSIFICATION OF:			**17.LIMITATION OF ABSTRACT**	**18.NUMBER OF PAGES**	**19a. NAME OF RESPONSIBLE PERSON**
a. REPORT	**b. ABSTRACT**	**c. THIS PAGE**			Muralidhar Rangaswamy
Unclassified	Unclassified	Unclassified	UU	12	**19b. TELEPHONE NUMBER** *(include area code)* N/A

Standard Form 298 (Rev. 8-98)
Prescribed by ANSI Std. Z39.18

Indirect Dominant Mode Rejection: A Solution to Low Sample Support Beamforming

Ernesto L. Santos, Michael D. Zoltowski, *Fellow, IEEE*, and Muralidhar Rangaswamy, *Fellow, IEEE*

***Abstract*—Under conditions of low sample support, a low-rank solution of the minimum variance distortionless response (MVDR) equations can yield a higher output signal-to-interference-plus-noise ratio (SINR) than the full-rank MVDR beamformer. In this paper, we investigate several low-rank beamforming techniques, and we also propose a new beamformer that we refer to as the indirect dominant mode rejection (IDMR). We analyze the degradation in the output SINR caused by residual cross correlations embedded in the sampled covariance matrix due to low sample support. The IDMR beamformer is based on a parametric estimate of the covariance matrix, in which any cross correlation is canceled out. Simulations reveal that the IDMR beamformer yields a dramatic improvement in output SINR relative to the conjugate gradient (CG), principal component inverse (PCI), and dominant mode rejection (DMR) beamformers. In our investigation of the low-rank CG beamformer, we address the issue of whether the unity gain constraint in the look direction should be enforced *a priori* via the use of a blocking matrix or effected *a posteriori* through simple scaling of the beamforming vector. Remarkably, it is proven that the two methods yield exactly the same low-rank beamformer at each and every rank.**

***Index Terms*—Blocking matrix, conjugate gradient beamformer, dominant mode rejection (DMR) beamformer, indirect dominant mode rejection (IDMR) beamformer, low sample support beamforming, minimum variance distortionless (MVDR) beamformer, robust adaptive beamforming.**

I. Introduction

ARRAYS of sensors have been widely used in wireless communications in a variety of applications such as sonar, radar, astronomy, medical imaging, sound processing, and seismic exploration. In this paper, we investigate several low-rank beamforming techniques, and we also propose a new beamforming technique that we refer to as indirect dominant mode rejection (IDMR) [1]. To maximize performance in a nonstationary scenario, adaptive beamforming (ABF) is necessary. In rapidly changing scenarios, only a limited number of snapshots is available to estimate the covariance matrix; under these circumstances, the low-rank minimum variance distortionless response (MVDR) equations yield faster convergence in terms of the signal-to-interference-plus-noise ratio (SINR) performance than the full-rank MVDR beamformer [2]–[5]. Owsley [6] introduced dominant mode rejection (DMR) low-rank ABF. Kirsteins and Tufts [7] introduced principal components inverse (PCI) low-rank ABF. Goldstein *et al.* [8] introduced the multistage Wiener filter (MWF), which was proven to be equivalent to the conjugate gradients (CG) ABF [9]. The performance of the aforementioned beamformers depends on the rank in which they operate. However, there is no robust algorithm to select the optimal rank because the true interference-plus-noise covariance matrix is not known. It is well known that the optimum rank is a function of the number of signal sources (dominant modes) and of the number of samples used to estimate the covariance matrix. Through simulations we also show that the optimum rank varies with the look direction [10], i.e., the optimal rank of operation is not necessarily the same for all the different signals. In the literature [6], [11], the DMR/PCI method is applied using all of the dominant eigenvectors of the covariance matrix. The number of dominant eigenvectors does not vary with look direction, and therefore does not affect all look directions with an optimal SINR. In our simulations, we show that the output SINR can undergo substantial variations, depending on the rank that is chosen. Consequently, the output SINR can be seriously degraded if the beamformer operates at an inadequate rank. To solve signal mismatch and low sample support problems, Vorobyov *et al.* proposed in [12] a robust adaptive beamforming algorithm using worst case performance optimization. Also dealing with signal mismatch and low sample support problems, Mestre and Lagunas in [13] propose an optimal diagonal loading technique. In this paper, we contribute to the ABF field by proposing the IDMR beamformer, which operates at its maximum rank with an output SINR very close to the maximum over all ranks. Also, the output SINR is significantly higher than the SINR obtained with existing ABF techniques.

The MVDR beamformer maximizes the output SINR only when the desired signal is uncorrelated to the interference. Due to finite sample averaging, residual correlations between sources are present in the sample covariance matrix, causing a degradation in the performance of MVDR-based beamformers. Even when all incident signals are truly uncorrelated, the sample signal-source covariance matrix intrinsically embedded in the sample spatial covariance matrix has substantial off-diagonal terms. This is especially true under conditions of low sample support, thereby giving the "appearance" of correlation between signals. This problem is circumvented in the IDMR algorithm proposed herein by forcing the correlation between

Manuscript received December 21, 2005; revised August 4, 2006. The associate editor coordinating the review of this manuscript and approving it for publication was Dr. Franz Hlawatsch. This research was supported by the Office of Naval Research under Grant Number N00014-04-1-0083. The work of M. Rangaswamy was supported by the Air Force Office of Scientific Research under project 2304.

E. L. Santos and M. D. Zoltowski are with the School of Electrical and Computer Engineering, Purdue University, West Lafayette, IN 47907 USA (e-mail: santose@ecn.purdue.edu; mikedz@ecn.purdue.edu).

M. Rangaswamy is with the Air Force Research Laboratory/SNHE, Hascom Air Force Base, MA 01731-2909 USA (e-mail: muralidhar. rangaswamy@hanscom.af.mil).

Color versions of one or more of the figures in this paper are available online at http://ieeexplore.ieee.org.

Digital Object Identifier 10.1109/TSP.2007.893926

signals to be zero in the parametrically constructed spatial covariance matrix estimate, which is then used in the computation of the MVDR beamformer. Through simulations, we show that under low sample support, the IDMR beamformer yields a substantially higher SINR than either the full-rank MVDR beamformer or low-rank MVDR beamformers such as CG and PCI/DMR, even when these low-rank beamformers operate at the optimal rank. We also show through simulations that when signals are truly correlated, the IDMR beamformer yields substantially higher SINR than the low-rank CG and PCI/DMR beamformers. Even though the IDMR beamformer was originally designed as a tool to circumvent residual signal-source correlation due to low sample support, it is also effective in the case where the sources are truly correlated.

The relationship between steering-independent ABF and steering-dependent ABF is investigated for the case of CG-based low-rank beamforming. The scenario assumes the formation of multiple adaptive beams, each pointed to a different look direction. In steering-dependent ABF, a generalized sidelobe canceler (GSC) [14] is formed for each look direction. Mathematically, the GSC serves to convert the constrained MVDR optimization problem to an unconstrained optimization problem, thereby enforcing *a priori* the unity gain constraint in the look direction. In contrast, in steering-independent ABF, an unscaled version of the Wiener–Hopf equations is solved, and the unity gain constraint is enforced *a posteriori* through simple scaling of the resulting ABF weight vector. Implementation of a GSC for each look direction requires the construction and application to the data of a blocking matrix for each look direction. The attendant computational complexity is quite substantial. In this paper, we prove a very important and somewhat surprising result: the low-rank beamformer obtained with steering-dependent (SD) conjugate gradients (SD-CG) is exactly the same as the low-rank beamformer obtained with steering-independent (SI) conjugate gradients (SI-CG) at any rank. Thus, the performance of SD-CG can be obtained without having to form blocking matrices for each look direction.

In Section II, we present the signal model. In Section III, we present some background on MVDR beamforming and provide an overview of the SI-CG and SD-CG beamformers. In Section IV, we prove the equivalence of the SI-CG and SD-CG beamformers. In Section V, we show the deterioration to MVDR-based beamformers caused by residual correlations, and we introduce the IDMR beamformer. In Section VI, we present the simulations where we compare the IDMR beamformer to the existing beamformers. In Section VII, we summarize the conclusions.

II. Signal Model

Consider an array of m sensors receiving signals from d sources of emission at directions θ_k, $k = 1, \ldots, d$ with respect to the broadside of the array. The angles of arrival are enumerated such that θ_1 is the angle of the desired source. We will assume that the desired source is narrowband and that the narrowband filtering about the center frequency of the desired source f_o occurs at the front end of the receiver such that the $(d-1)$ interfering signals are narrowband and colocated in frequency with the desired signal at the beamformer input. We will also assume additive noise at each sensor. Let $\mathbf{x}(t) = [x_1(t), x_2(t), \ldots, x_m(t)]^T$, where $x_i(t)$ is the signal received at the ith array element. $(.)^T$ denotes transpose. Given the above-assumed scenario, $\mathbf{x}(t)$ can be expressed in the following fashion:

$$\mathbf{x}(t) = \mathbf{A}\mathbf{s}(t) + \mathbf{n}(t). \tag{1}$$

$\mathbf{A} = [\mathbf{a}(\theta_1), \mathbf{a}(\theta_2), \ldots, \mathbf{a}(\theta_d)]$ is called the signal direction matrix (SDM), where $A_{ik} = a_i(\theta_k)$ is the response of the ith array element relative to that of the first element when a single signal arrives at θ_k, $\mathbf{s}(t) = [s_1(t), \ldots, s_d(t)]^T$, where $s_k(t)$ is the signal associated with the kth source as received at the first array element, and $\mathbf{n}(t) = [n_1(t), n_2(t), \ldots, n_m(t)]^T$, where $n_i(t)$ is the additive noise present at the ith array element.

The output of the beamformer is given by $y(t) = \mathbf{w}^H\mathbf{x}(t)$, where $\mathbf{w} = [w_1, w_2, \ldots, w_m]^T$ is the beamformer weight vector. $(.)^H$ denotes Hermitian (conjugate) transpose.

III. MVDR Beamforming

After beamforming, the output SINR can be expressed as [12], [15]

$$\begin{aligned}\text{SINR} &= \frac{E\left\{\left|\mathbf{w}^H\mathbf{a}_1 s_1(t)\right|^2\right\}}{E\left\{\left|\mathbf{w}^H\left[\mathbf{x}(t) - \mathbf{a}_1 s_1(t)\right]\right|^2\right\}} \\ &= \frac{\sigma_1^2|\mathbf{w}^H\mathbf{a}_1|^2}{\mathbf{w}^H\mathbf{R}_{i+n}\mathbf{w}}\end{aligned} \tag{2}$$

where

$$\mathbf{R}_{i+n} = E\left\{\left[\mathbf{x}(t) - \mathbf{a}_1 s_1(t)\right]\left[\mathbf{x}(t) - \mathbf{a}_1 s_1(t)\right]^H\right\} \tag{3}$$

is the interference-plus-noise covariance matrix, and $\sigma_1^2 = E\{|s_1(t)|^2\}$ is the power of the desired signal. Maximizing (2) is equivalent to minimizing 1/SINR, as follows:

$$\min_{\mathbf{w}} \quad \frac{\mathbf{w}^H\mathbf{R}_{i+n}\mathbf{w}}{\sigma_1^2|\mathbf{w}^H\mathbf{a}_1|^2}. \tag{4}$$

Observing that the cost function above is unaltered when $\mathbf{w}$ is scaled, we can impose, without a loss of generality, the constraint $\mathbf{w}^H\mathbf{a}_1 = 1$, which can always be achieved by scaling $\mathbf{w}$. Hence, the maximization of the output SINR is equivalent to

$$\begin{aligned}\min_{\mathbf{w}} \quad & \mathbf{w}^H\mathbf{R}_{i+n}\mathbf{w} \\ \text{subject to}: \quad & \mathbf{w}^H\mathbf{a}_1 = 1.\end{aligned} \tag{5}$$

The solution to (5) is the well-known MVDR beamformer, given by solving

$$\mathbf{R}_{i+n}\mathbf{w} = \lambda\mathbf{a}_1 \tag{6}$$

where λ serves to satisfy the unity gain constraint in (5).

In many practical applications, the ideal signal-free covariance matrix $\mathbf{R}_{i+n}$ is unavailable, and a sample estimate from N snapshots

$$\hat{\mathbf{R}} = \frac{1}{n}\sum_{t=1}^{n}\mathbf{x}(t)\mathbf{x}^H(t) \tag{7}$$

is often used instead of $\mathbf{R}_{i+n}$. It is observed that if the desired signal is uncorrelated to the interference and to the array noise, then

$$\begin{aligned} \min_{\mathbf{w}} \quad & \mathbf{w}^H\mathbf{R}\mathbf{w} \\ \text{subject to}: \quad & \mathbf{w}^H\mathbf{a}_1 = 1 \end{aligned} \tag{8}$$

where

$$\mathbf{R} = E\left\{\mathbf{x}(t)\mathbf{x}^H(t)\right\} \tag{9}$$

is equivalent to the minimization problem of (5). Observe that under the constraint $\mathbf{w}^H\mathbf{a}_1 = 1$

$$\begin{aligned} \min_{\mathbf{w}} \mathbf{w}^H\mathbf{R}_{i+n}\mathbf{w} &= \min_{\mathbf{w}} \mathbf{w}^H E \\ &\quad \times \Big\{ [\mathbf{A}\mathbf{s}(t) - \mathbf{a}_1 s_1(t) + \mathbf{n}(t)] \\ &\quad\quad \times [\mathbf{A}\mathbf{s}(t) - \mathbf{a}_1 s_1(t) + \mathbf{n}(t)]^H \Big\} \mathbf{w} \\ &= \min_{\mathbf{w}} \left\{ \mathbf{w}^H\mathbf{R}\mathbf{w} - \sigma_1^2 |\mathbf{w}^H\mathbf{a}_1|^2 \right\} \\ &= \min_{\mathbf{w}} \mathbf{w}^H\mathbf{R}\mathbf{w}. \end{aligned} \tag{10}$$

Hence, when the desired signal is uncorrelated to the interference and to the array noise, minimizing $\mathbf{w}^H\mathbf{R}_{i+n}\mathbf{w}$ subject to $\mathbf{w}^H\mathbf{a}_1 = 1$ is the same as minimizing $\mathbf{w}^H\mathbf{R}\mathbf{w}$ subject to $\mathbf{w}^H\mathbf{a}_1 = 1$; and, therefore, the MVDR beamformer with either $\mathbf{R}_{i+n}$ or $\mathbf{R}$ maximizes the output SINR. It is important to note that this only happens when the true covariance matrix is known and the desired signal is uncorrelated to the interference and to the array noise. Even when sources are truly uncorrelated, residual correlations arise due to finite sample averaging, causing the output SINR to be significantly degraded, since minimizing $\mathbf{w}^H\hat{\mathbf{R}}\mathbf{w}$ is not tantamount to minimizing $\mathbf{w}^H\hat{\mathbf{R}}_{i+n}\mathbf{w}$. This motivates us to introduce IDMR beamforming, which is based on a parametric estimate of the correlation matrix where the residual correlations are canceled out. The IDMR beamformer is presented in Section V.

Low-rank MVDR steering-independent beamformers arise when a a low-rank solution for (6) is used. SI-CG consists of using the CG algorithm [16] to solve (6); this solution is obtained by minimizing the quadratic function

$$f(\mathbf{w}) = \frac{1}{2}\mathbf{w}^H\mathbf{R}\mathbf{w} - \mathbf{w}^H\mathbf{a}_1. \tag{11}$$

Steering-dependent ABF consists of enforcing the unity gain constraint *a priori* through the use of a blocking matrix $\mathbf{B}$ and thus transforming the constrained optimization problem of (5) in an unconstrained optimization problem. The columns of $\mathbf{B}$ form an orthonormal basis for the orthogonal complement of the steering vector $\mathbf{a}_1$. While $\mathbf{B}$ is not unique, it must satisfy

$$\begin{aligned} &\mathcal{R}(\mathbf{B}) = \mathbf{a}_1^{\perp} \\ &\mathbf{B}^H\mathbf{B} = \mathbf{I} \end{aligned} \tag{12}$$

where the operator $\mathcal{R}$ denotes range of a matrix, and $\mathbf{I}$ denotes the identity matrix. There are several forms to find a blocking matrix $\mathbf{B}$; computation through a Householder transformation is shown in the Appendix. Expressing $\mathbf{w}$ as

$$\mathbf{w} = \frac{1}{m}(\mathbf{a}_1 + \mathbf{B}\mathbf{u}) \tag{13}$$

guarantees that the unity gain constraint is satisfied *a priori*.

Substituting (13) into (5) leads to the unconstrained optimization problem

$$\min_{\mathbf{u}} \frac{1}{m^2}(\mathbf{a}_1 + \mathbf{B}\mathbf{u})^H\mathbf{R}(\mathbf{a}_1 + \mathbf{B}\mathbf{u}). \tag{14}$$

Taking the gradient of (14) with respect to $\mathbf{u}$ dictates that the optimal value of $\mathbf{u}$ is the solution to

$$(\mathbf{B}^H\mathbf{R}\mathbf{B})\mathbf{u} = -\mathbf{B}^H\mathbf{R}\mathbf{a}_1. \tag{15}$$

Low-rank-MVDR-steering-dependent adaptive beamforming methods consist of using a low-rank solution for (15) and substituting it in (13). When the full-rank solution is taken, both solutions of (6) and (13), SI and SD beamforming, respectively, yield the same weight vector $\mathbf{w}$. When a low-rank solution is used, the low-rank SI and SD weight vectors are not guaranteed to be equal.

IV. Equivalence Between SI-CG and SD-CG

In the SI-CG beamformer, the CG algorithm is used to solve (6), note that (see [17] and [18]) at step r, the output vector of the CG algorithm $\mathbf{w}'^{(r)}$ minimizes the $\mathbf{R}$-norm of the error, which is given by

$$e_{si}\left(\mathbf{w}'^{(r)}\right) = \left(\mathbf{w}'^{(r)} - \mathbf{R}^{-1}\mathbf{a}_1\right)^H \mathbf{R} \left(\mathbf{w}'^{(r)} - \mathbf{R}^{-1}\mathbf{a}_1\right) \tag{16}$$

subjected to $\mathbf{w}'^{(r)}$ being constrained within the Krylov subspace $\mathcal{K}_{si}^{(r)}$, defined by the column space of $\mathbf{K}_{si}^{(r)}$ below:

$$\mathbf{K}_{si}^{(r)} = [\mathbf{a}_1 \vdots \mathbf{R}\mathbf{a}_1 \vdots \ldots \vdots \mathbf{R}^{r-1}\mathbf{a}_1]. \tag{17}$$

It follows from [9] that after r steps of CG, the solution is constrained to lie in a r-dimensional Krylov subspace. Thus, it is referred to as a rank r solution.

For the purposes of comparing the performance of SD-CG relative to SI-CG, we desire that the rank-one solution for both methods be the scaled steering vector $(1/m)\mathbf{a}_1$, which is tantamount to the CBF. Thus, for SD-CG, $(r-1)$ steps of CG are taken in solving (15) to obtain the solution denoted $\mathbf{u}^{(r-1)}$. Substituting $\mathbf{u}^{(r-1)}$ for $\mathbf{u}$ into (13) yields the rank r SD-CG beamformer denoted $\mathbf{w}_{sd}^{(r)}$.

Similarly to $\mathbf{w}'^{(r)}$, $\mathbf{u}^{(r-1)}$ is restricted to lie in the Krylov subspace $\mathcal{K}_u^{(r-1)}$ defined by the range space of the matrix $\mathbf{K}_u^{(r-1)}$, where $\mathbf{K}_u^{(r)}$ is defined as

$$\mathbf{K}_u^{(r)} = \Big[\mathbf{B}^H\mathbf{R}\mathbf{a}_1 \vdots (\mathbf{B}^H\mathbf{R}\mathbf{B})\mathbf{B}^H\mathbf{R}\mathbf{a}_1 \vdots \cdots \vdots (\mathbf{B}^H\mathbf{R}\mathbf{B})^{r-1}\mathbf{B}^H\mathbf{R}\mathbf{a}_1\Big].$$

In turn, (13) and the equation above dictate that $\mathbf{w}_{sd}^{(r)}$ is restricted to lie in the range space of the matrix

$$\mathbf{K}_{sd}^{(r)} = \left[\mathbf{a}_1 \vdots \mathbf{B}\mathbf{K}_u^{(r-1)}\right]. \tag{18}$$

Simple algebraic manipulation leads to the following expression for the Krylov subspace $\mathcal{K}_{sd}^{(r)}$ represented by the range space of

$$\mathbf{K}_{sd}^{(r)} = \left[\mathbf{a}_1 \vdots (\mathbf{B}\mathbf{B}^H\mathbf{R})\mathbf{a}_1 \vdots \ldots \vdots (\mathbf{B}\mathbf{B}^H\mathbf{R})^{r-1}\mathbf{a}_1\right]. \tag{19}$$

The following theorem states that the SD-CG and SI-CG Krylov subspaces of dimension r are the same.

Theorem 1:

$$\operatorname{span}\{\mathbf{a}_1, \mathbf{R}\mathbf{a}_1, \ldots, \mathbf{R}^r\mathbf{a}_1\} = \operatorname{span}\{\mathbf{a}_1, (\mathbf{B}\mathbf{B}^H\mathbf{R})\mathbf{a}_1, \ldots, (\mathbf{B}\mathbf{B}^H\mathbf{R})^r\mathbf{a}_1\}, \quad r = 1, 2, \ldots, m.$$

Proof is by induction. The basis case is proven in step 1, and the induction step is proven in step 2 below.

1) Basis case:

$$\operatorname{span}\{\mathbf{a}_1, \mathbf{R}\mathbf{a}_1\} = \operatorname{span}\{\mathbf{a}_1, \mathbf{B}\mathbf{B}^H\mathbf{R}\mathbf{a}_1\}.$$

Proof:

i) $[\mathbf{a}_1 \vdots \mathbf{B}]$ is an orthonormal basis for $\mathcal{R}^m$ since $\mathbf{B}$ is the orthogonal complement of $\mathbf{a}_1$ by construction, and the columns of $\mathbf{B}$ are orthonormal. $\mathbf{B}\mathbf{B}^H$ is a projection matrix.

$$\therefore \exists\beta | \mathbf{R}\mathbf{a}_1 = \beta\mathbf{a}_1 + \mathbf{B}\mathbf{B}^H\mathbf{R}\mathbf{a}_1.$$

ii) $\operatorname{span}\{\mathbf{a}_1, \mathbf{R}\mathbf{a}_1\} = \operatorname{span}\{\mathbf{a}_1, \beta\mathbf{a}_1 + \mathbf{B}\mathbf{B}^H\mathbf{R}\mathbf{a}_1\} = \operatorname{span}\{\mathbf{a}_1, \mathbf{B}\mathbf{B}^H\mathbf{R}\mathbf{a}_1\}$ ■

2) Inductive step:

Define $\mathbf{C} = \mathbf{B}\mathbf{B}^H\mathbf{R}$.

If $\operatorname{span}\{\mathbf{a}_1, \mathbf{R}\mathbf{a}_1, \ldots, \mathbf{R}^r\mathbf{a}_1\} = \operatorname{span}\{\mathbf{a}_1, \mathbf{C}\mathbf{a}_1, \ldots, \mathbf{C}^r\mathbf{a}_1\}$, then $\operatorname{span}\{\mathbf{a}_1, \mathbf{R}\mathbf{a}_1, \ldots, \mathbf{R}^{r+1}\mathbf{a}_1\} = \operatorname{span}\{\mathbf{a}_1, \mathbf{C}\mathbf{a}_1, \ldots, \mathbf{C}^{r+1}\mathbf{a}_1\}$

Proof:

i)

$$\begin{aligned}
&\forall\, j > 0, \exists\beta_j | \mathbf{R}^j\mathbf{a}_1 \\
&\quad = \beta_j\mathbf{a}_1 + \mathbf{B}\mathbf{B}^H\mathbf{R}^j\mathbf{a}_1, \\
&\forall k > 0,\ \operatorname{span}\{\mathbf{a}_1, \mathbf{R}\mathbf{a}_1, \ldots, \mathbf{R}^k\mathbf{a}_1\} \\
&\quad = \operatorname{span}\{\mathbf{a}_1, \beta_1\mathbf{a}_1 + \mathbf{B}\mathbf{B}^H\mathbf{R}\mathbf{a}_1, \\
&\qquad \ldots, \beta_k\mathbf{a}_1 + \mathbf{B}\mathbf{B}^H\mathbf{R}^k\mathbf{a}_1\} \\
&\quad = \operatorname{span}\{\mathbf{a}_1, \mathbf{B}\mathbf{B}^H\mathbf{R}\mathbf{a}_1, \ldots, \mathbf{B}\mathbf{B}^H\mathbf{R}^k\mathbf{a}_1\}.
\end{aligned}$$

ii)

$$\begin{aligned}
&\mathbf{C}^{r+1}\mathbf{a}_1 \\
&\quad = \mathbf{C}(\mathbf{C}^r\mathbf{a}_1) \\
&\quad = \mathbf{C}\Big(\sum_{i=0}^{r}\alpha_i\mathbf{R}^i\mathbf{a}_1\Big), \text{ by induction hypothesis} \\
&\quad = \sum_{i=0}^{r}\alpha_I\mathbf{B}\mathbf{B}^H\mathbf{R}^{i+1}\mathbf{a}_1.
\end{aligned}$$

iii)

$$\begin{aligned}
&\operatorname{span}\{\mathbf{a}_1, \mathbf{C}\mathbf{a}_1, \ldots, \mathbf{C}^r\mathbf{a}_1, \mathbf{C}^{r+1}\mathbf{a}_1\} \\
&\quad = \operatorname{span}\{\mathbf{a}_1, \mathbf{R}\mathbf{a}_1, \ldots, \mathbf{R}^r\mathbf{a}_1, \mathbf{C}^{r+1}\mathbf{a}_1\}, \\
&\qquad \text{by induction hypothesis} \\
&\quad = \operatorname{span}\{\mathbf{a}_1, \mathbf{B}\mathbf{B}^H\mathbf{R}\mathbf{a}_1, \ldots, \mathbf{B}\mathbf{B}^H\mathbf{R}^r\mathbf{a}_1, \\
&\qquad \sum_{i=0}^{r}\alpha_i\mathbf{B}\mathbf{B}^H\mathbf{R}^{i+1}\mathbf{a}_1\}, \text{ by i) and ii)} \\
&\quad = \operatorname{span}\{\mathbf{a}_1, \mathbf{B}\mathbf{B}^H\mathbf{R}\mathbf{a}_1, \\
&\qquad \ldots, \mathbf{B}\mathbf{B}^H\mathbf{R}^r\mathbf{a}_1, \mathbf{B}\mathbf{B}^H\mathbf{R}^{r+1}\mathbf{a}_1\} \\
&\quad = \operatorname{span}\{\mathbf{a}_1, \mathbf{R}\mathbf{a}_1, \ldots, \mathbf{R}^r\mathbf{a}_1, \mathbf{R}^{r+1}\mathbf{a}_1\}, \text{ by i).}
\end{aligned}$$

Proof: ■

Thus, the rank r SI-CG and SD-CG beamformers are constrained to lie in the same subspaces.

A. Closed-Form Expressions for $\mathbf{w}_{si}^{(r)}$

Since we have proved that the rank r beamformers for SI-CG and SD-CG lie in the same subspace, the unscaled (prior to scaling to satisfy the unity gain constraint) SI-CG beamformer $\mathbf{w}_{si}^{\prime(r)}$ may be expressed as

$$\begin{aligned}
\mathbf{w}_{si}^{\prime(r)} &= \mathbf{K}_{si}^{(r)}\mathbf{y}^{(r)} \\
&= \mathbf{K}_{sd}^{(r)}\mathbf{x}^{(r)}
\end{aligned} \tag{20}$$

where $\mathbf{y}^{(r)}$ and $\mathbf{x}^{(r)}$ are $r \times 1$ vectors whose elements combine the columns of $\mathbf{K}_{si}$ and $\mathbf{K}_{sd}$, respectively. At this point, we seek a closed-form expression for $\mathbf{x}^{(r)}$, with $\mathbf{K}_{sd}^{(r)}$ given by (19). With this, the rank r SI-CG beamformer is expressed in the Krylov basis of the SD-CG beamformer. Later, we find a closed-form expression for the rank r SD-CG beamformer in the same basis. We can then easily compare the SI-CG and SD-CG beamformers.

The value of $\mathbf{x}^{(r)}$ is obtained by substituting $\mathbf{w}_{si}^{\prime(r)} = \mathbf{K}_{sd}^{(r)}\mathbf{x}^{(r)}$ into the objective function in (16) and noting that $\mathbf{x}^{(r)}$ minimizes the function. Subsequently, taking the gradient and setting it to zero yields

$$\begin{aligned}
&\mathbf{K}_{sd}^{(r)H}\mathbf{R}\mathbf{K}_{sd}^{(r)}\mathbf{x}^{(r)} - \mathbf{K}_{sd}^{(r)H}\mathbf{a}_1 = \mathbf{0} \\
&\qquad \Rightarrow\ \mathbf{x}^{(r)} = \left(\mathbf{K}_{sd}^{(r)H}\mathbf{R}\mathbf{K}_{sd}\right)^{-1}\mathbf{K}_{sd}^{(r)H}\mathbf{a}_1.
\end{aligned} \tag{21}$$

Substituting the expression for $\mathbf{K}_{sd}^{(r)}$ in (18), the inverse of $\mathbf{K}_{sd}^{(r)H}\mathbf{R}\mathbf{K}_{sd}^{(r)}$ may be expressed as

$$\begin{aligned}
&\left(\mathbf{K}_{sd}^{(r)H}\mathbf{R}\mathbf{K}_{sd}^{(r)}\right)^{-1} \\
&= \begin{bmatrix} \mathbf{a}_1^H\mathbf{R}\mathbf{a}_1 & \mathbf{a}_1^H\mathbf{R}\mathbf{B}\mathbf{K}_u^{(r-1)} \\ \mathbf{K}_u^{(r-1)H}\mathbf{B}^H\mathbf{R}\mathbf{a}_1 & \mathbf{K}_u^{(r-1)H}\mathbf{B}^H\mathbf{R}\mathbf{B}\mathbf{K}_u^{(r-1)} \end{bmatrix}^{-1}.
\end{aligned} \tag{22}$$

In addition, it follows that

$$\mathbf{K}_{sd}^{(r)H}\mathbf{a}_1 = [1 \vdots \mathbf{0}]^H. \tag{23}$$

Substituting (22) and (23) into (21) dictates that only the first column of the inverse matrix in (22) is needed. Invoking the block matrix inversion lemma, $\mathbf{x}^{(r)}$ may be computed as

$$\mathbf{x}^{(r)} = \gamma \begin{bmatrix} 1 \\ -\left(\mathbf{K}_u^{(r-1)H}\mathbf{B}^H\mathbf{R}\mathbf{B}\mathbf{K}_u^{(r-1)}\right)^{-1}\mathbf{K}_u^{(r-1)H}\mathbf{B}\mathbf{R}\mathbf{a}_1 \end{bmatrix} \tag{24}$$

where γ is a multiplicative scalar that will be accounted for when the unity gain constraint is satisfied. Substituting (24) into (20), with $\mathbf{K}_{sd}^{(r)}$ given by (18), yields

$$\mathbf{w}_{si}'^{(r)} = \gamma\left(\mathbf{a}_1 - \mathbf{B}\mathbf{K}_u^{(r-1)}\left(\mathbf{K}_u^{(r-1)H}\mathbf{B}^H\mathbf{R}\mathbf{B}\mathbf{K}_u^{(r-1)}\right)^{-1} \times\mathbf{K}_u^{(r-1)H}\mathbf{B}\mathbf{R}\mathbf{a}_1\right). \tag{25}$$

Since the columns of $\mathbf{B}$ are orthogonal to $\mathbf{a}_1$ by construction, scaling to satisfy the unity gain constraint simply implies

$$\mathbf{w}_{si}^{(r)} = \frac{1}{m}\left[\mathbf{a}_1 - \mathbf{B}\mathbf{K}_u^{(r-1)}\left(\mathbf{K}_u^{(r-1)H}\mathbf{B}^H\mathbf{R}\mathbf{B}\mathbf{K}_u^{(r-1)}\right)^{-1} \times\mathbf{K}_u^{(r-1)H}\mathbf{B}\mathbf{R}\mathbf{a}_1\right]. \tag{26}$$

B. Closed-Form Expressions for $\mathbf{w}_{sd}^{(r)}$

According to (13), the rank r SD-CG beamformer may be expressed as

$$\begin{aligned}\mathbf{w}_{sd}^{(r)} &= \frac{1}{m}\left[\mathbf{a}_1 + \mathbf{B}\mathbf{u}^{(r-1)}\right] \\ &= \frac{1}{m}\left[\mathbf{a}_1 + \mathbf{B}\mathbf{K}_u^{(r-1)}\mathbf{z}^{(r-1)}\right].\end{aligned} \tag{27}$$

Since $\mathbf{u}^{(r-1)}$ is determined by solving (15) via the CG algorithm, it is the vector that minimizes the objective function

$$e_{sd}\left(\mathbf{u}^{(r-1)}\right) = \left(\mathbf{u}^{(r-1)} + \left(\mathbf{B}^H\mathbf{R}\mathbf{B}\right)^{-1}\mathbf{B}^H\mathbf{R}\mathbf{a}_1\right)^H \times\mathbf{B}^H\mathbf{R}\mathbf{B}\left(\mathbf{u}^{(r-1)} + \left(\mathbf{B}^H\mathbf{R}\mathbf{B}\right)^{-1}\mathbf{B}^H\mathbf{R}\mathbf{a}_1\right) \tag{28}$$

with $\mathbf{u}^{(r-1)}$ constrained to lie in the range space of the matrix $\mathbf{K}_u^{(r-1)}$ in (18). Substituting $\mathbf{K}_u^{(r-1)}\mathbf{z}^{(r-1)}$ for $\mathbf{u}^{(r-1)}$ above dictates that $\mathbf{z}^{(r-1)}$ is the vector that minimizes

$$\begin{aligned}&\mathbf{z}^{(r-1)H}\mathbf{K}_u^{(r-1)H}\mathbf{B}^H\mathbf{R}\mathbf{B}\mathbf{K}_u^{(r-1)}\mathbf{z}^{(r-1)} \\ &\quad+\mathbf{z}^{(r-1)H}\mathbf{K}_u^{(r-1)H}\mathbf{B}^H\mathbf{R}\mathbf{a}_1 + \mathbf{a}_1^H\mathbf{R}\mathbf{B}\mathbf{K}_u^{(r-1)}\mathbf{z}^{(r-1)}\end{aligned}$$

where we have omitted an inconsequential additive constant. Taking the gradient with respect to $\mathbf{n}^{(r-1)}$ and setting it to zero yields

$$\mathbf{z}^{(r-1)} = -\left(\mathbf{K}_u^{(r-1)H}\mathbf{B}^H\mathbf{R}\mathbf{B}\mathbf{K}_u^{(r-1)}\right)^{-1}\mathbf{K}_u^{(r-1)H}\mathbf{B}^H\mathbf{R}\mathbf{a}_1. \tag{29}$$

In turn, substituting $\mathbf{z}^{(r-1)}$ back into (27) yields

$$\mathbf{w}_{sd}^{(r)} = \frac{1}{m}\left[\mathbf{a}_1 - \mathbf{B}\mathbf{K}_u^{(r-1)}\left(\mathbf{K}_u^{(r-1)H}\mathbf{B}^H\mathbf{R}\mathbf{B}\mathbf{K}_u^{(r-1)}\right)^{-1} \times\mathbf{K}_u^{(r-1)H}\mathbf{B}^H\mathbf{R}\mathbf{a}_1\right]. \tag{30}$$

Equations (26) and (30) are observed to be identical, thereby proving that the rank r SI-CG beamformer is equal to the rank r SD-CG beamformer. Brennan, Mallett, and Reed have shown in [19] that the full-rank MVDR steering-dependent beamformer implemented through a sidelobe cancellation [14] and the full-rank MVDR steering independent beamformer converge to the same beamformer. We showed that when implemented through CG the low-rank versions of these beamformer also yield the same beamformer at every rank.

V. Indirect DMR

In Section II, we showed that when the desired signal is uncorrelated to the interference, the MVDR beamformer maximizes the output SINR. This is true even when the desired signal is present in the covariance matrix, as long as the true correlation matrix is available. If the desired signal is correlated with the interference, then the MVDR beamformer no longer maximizes the output SINR. Even when the desired signal and the interference are not correlated, the covariance matrix estimated from a limited number of snapshots contains residual correlation. Under these circumstances, the MVDR beamformer does not maximize the output SINR [20].

As an example, we consider the case in which two uncorrelated signals are arriving at the array. To facilitate the analysis, we do not include the effects of the array noise. The signal arriving at the array is given by

$$\mathbf{x}(t) = s_1(t)\mathbf{a}_1 + s_2(t)\mathbf{a}_2 \tag{31}$$

where $s_1(t)$ and $s_2(t)$ are independent complex Gaussian random processes. The sample covariance matrix from n samples is given by

$$\begin{aligned}&\frac{1}{n}\sum_{t=1}^{n}\mathbf{x}(t)\mathbf{x}^H(t) = [\mathbf{a}_1\ \mathbf{a}_2] \\ &\times\begin{bmatrix} n^{-1}\sum_{t=1}^{n}|s_1(t)|^2 & n^{-1}\sum_{t=1}^{n}s_1(t)s_2^*(t) \\ n^{-1}\sum_{t=1}^{n}s_2(t)s_1^*(t) & n^{-1}\sum_{t=1}^{n}|s_2(t)|^2 \end{bmatrix}\begin{bmatrix}\mathbf{a}_1^H \\ \mathbf{a}_2^H\end{bmatrix}.\end{aligned} \tag{32}$$

The nondiagonal terms in the signal-source covariance matrix (SSCM), which is represented by the matrix in the middle, converge to zero as $n \to \infty$. This is proved by observing that the mean of these nondiagonal terms is zero

$$E\left\{\frac{1}{n}\sum_{t=1}^{n}s_2(t)s_1^*(t)\right\} = 0 \tag{33}$$

and the variance goes to zero as $n \to \infty$

$$E\left\{\frac{1}{n^2}\sum_{t=1}^{n}s_2(t)s_1^*(t)\sum_{t'=1}^{n}s_2^*(t')s_1(t')\right\} = \frac{\sigma_1^2\sigma_2^2}{n} \tag{34}$$

where $\sigma_1^2 = E\{|s_1(t)|^2\}$ and $\sigma_2^2 = E\{|s_1(t)|^2\}$.

Since the variance of the nondiagonal terms go to zero relatively slowly (proportional to $1/n$), under low sample support, these terms can significantly deteriorate the output SINR obtained with MVDR beamforming. This motivates us to propose the IDMR beamformer, which is based on a parametric estimate

TABLE I
OUTLINE OF THE IDMR ALGORITHM

i	Estimate the directions of the dominant sources and form $\hat{\mathbf{A}}$.
ii	Estimate σ_n^2.
iii	Compute $\hat{\mathbf{P}}_d = \text{diag}\left(\hat{\mathbf{A}}^{\dagger}(\hat{\mathbf{R}} - \hat{\sigma}_n^2\mathbf{I})\hat{\mathbf{A}}^{\dagger H}\right)$.
iv	Parametrically form $\mathbf{R}_{idmr} = \hat{\mathbf{A}}\hat{\mathbf{P}}_d\hat{\mathbf{A}}^H + \hat{\sigma}_n^2\mathbf{I}$.
v	Compute $\mathbf{w}_{idmr} = (\mathbf{a}_1^H\mathbf{R}_{idmr}^{-1}\mathbf{a}_1)^{-1}\mathbf{R}_{idmr}^{-1}\mathbf{a}_1$

of the covariance matrix in which the embedded residual correlations are canceled out. In the derivation of the IDMR beamformer, we assume that the array manifold is known. In some practical applications, there is an error in the estimate of the array manifold. IDMR beamforming in the presence of array manifold mismatch will be considered in future work.

Substituting (1) into (9) and assuming that $\mathbf{s}(t)$ and $\mathbf{n}(t)$ are uncorrelated and $E\{\mathbf{n}(t)\mathbf{n}^H(t)\} = \sigma_n^2\mathbf{I}$, where σ_n^2 is the power of the noise at each array element, then the true covariance matrix $\mathbf{R}$ can be given by

$$\mathbf{R} = \mathbf{APA}^H + \sigma_n^2\mathbf{I} \tag{35}$$

where the matrix $\mathbf{P}$ is the signal source covariance matrix and is given by

$$\mathbf{P} = E\left\{\mathbf{s}(t)\mathbf{s}^H(t)\right\}. \tag{36}$$

In the IDMR beamformer, we propose to use

$$\hat{\mathbf{P}}_d = \text{diag}\left(\hat{\mathbf{A}}^{\dagger}\left(\hat{\mathbf{R}} - \hat{\sigma}_n^2\mathbf{I}\right)\hat{\mathbf{A}}^{\dagger H}\right) \tag{37}$$

as an estimate of the diagonalized signal source covariance matrix, where $\hat{\mathbf{A}}^{\dagger} = \left(\hat{\mathbf{A}}^H\mathbf{A}\right)^{-1}\hat{\mathbf{A}}^H$ is the pseudoinverse of $\hat{\mathbf{A}}$. $\hat{\mathbf{A}}$ is formed from the estimated signal directions, given the known form of the array manifold, and $\hat{\sigma}_n^2$ is an estimate of the noise variance. The nondiagonal elements of $\hat{\mathbf{P}}$, arising from residual correlations among sources due to finite sample averaging (or even due to true correlation among sources) are discarded, giving rise to a diagonalized signal-source covariance matrix estimate denoted $\hat{\mathbf{P}}_d$. Note from Section II that the nondiagonal elements cause the MVDR beamformer to not maximize the output SINR. Thus, even when sources are truly correlated, discarding these terms allows the MVDR beamformer to maximize the output SINR.

To compute $\hat{\mathbf{A}}$ the directions-of-arrival of the signals arriving at the array need to be estimated. At the expense of more computational processing, a high-resolution estimation of the dominant directions can be obtained applying MUSIC [21]; with considerably less computation, a lower resolution estimation can be obtained with the CBF.

Substituting $\hat{\mathbf{A}}$, $\hat{\mathbf{P}}_d$, $\hat{\sigma}_n^2$ into (35) yields a parametric estimate of the covariance matrix denoted $\mathbf{R}_{\text{idmr}}$. To avoid the look-direction mismatch a signal in the vicinity of the look direction should not be included in the formation of $\mathbf{R}_{\text{idmr}}$. The MVDR beamformer for the signal $s_1(t)$ is then formed using $\mathbf{R}_{\text{idmr}}$ as

$$\mathbf{w}_{idmr} = \frac{\mathbf{R}_{idmr}^{-1}\mathbf{a}_1}{\mathbf{a}_1^H\mathbf{R}_{idmr}^{-1}\mathbf{a}_1}. \tag{38}$$

Table I outlines the IDMR algorithm.

TABLE II
DIRECTIONS AND SNRS OF INCIDENT SIGNALS

Angle (dg)	-52	-35	0	7	12	48
SNR (dB)	16.2	16.2	-3.8	16.2	16.2	16.2

The underlying idea of the indirect-DMR technique proposed herein is to form a parametric estimate of the covariance matrix given information on the location and power of the *dominant* interferers previously obtained from either MUSIC or the CBF. With this parametric estimate of the covariance matrix where the cross correlations are removed, the MVDR beamformer maximizes the output SINR, by effectively allocating nulls at the positions of the dominant interferers. It is important to note that low power interferers are not important when forming the parametric covariance matrix $\mathbf{R}_{\text{idmr}}$, since it is not important to form nulls toward them. Thus, the performance of the IDMR beamformer is not compromised if weak sources are not detected by the MUSIC algorithm.

There are several works that focus on adaptive beamforming with low sample support. Diagonal loading of the sample covariance matrix has been extensively used in adaptive beamforming, however there has always been the issue of determining the optimal load. Mestre and Lagunas in [13] proposed a technique that optimizes diagonal loading. In the IDMR algorithm, there is also some reduced diagonal loading in the parametrically formed covariance matrix $\mathbf{R}_{\text{idmr}}$ (see Table I). Vorobyov *et al.* proposed in [12] a robust adaptive beamforming algorithm using worst case performance optimization. In Section VI, we compared the performance of IDMR to the performance obtained with Vorobyov's beamformer.

VI. SIMULATION RESULTS

Simulations were conducted employing a uniform and linear array of $m = 24$ elements with half-wavelength spacing receiving plane-wave signals. In the simulations, perfect knowledge of the array manifold was assumed, that is, no steering vector mismatch was considered. It is relevant to note that perfect knowledge of the array manifold does not imply perfect knowledge of the matrix $\mathbf{A}$. To estimate $\mathbf{A}$, it is also necessary to know the directions-of-arrival (DOAs) of the interference signals, and in the simulations, the interference DOAs are estimated. The noise at each array element is spatially and temporally white Gaussian. The incident signals are modeled as narrowband with amplitudes modeled as complex Gaussian random processes. We considered a scenario with six uncorrelated incident signals with arrival directions (in degrees) and respective signal-to-noise ratios (SNRs) (in decibels) at each array element as shown in Table II.

Fig. 1 shows the output SINR versus the rank of the beamformer for the signals at 0° and 7°; the SINR plotted is the average over 200 Monte Carlo simulation runs. The beamformers employed were the SI-CG, SD-CG, and DMR. The DMR beamformer requires an estimate of the array noise power, and since this beamformer is included with the only purpose to serve as a reference, the true value of the noise power is used as its

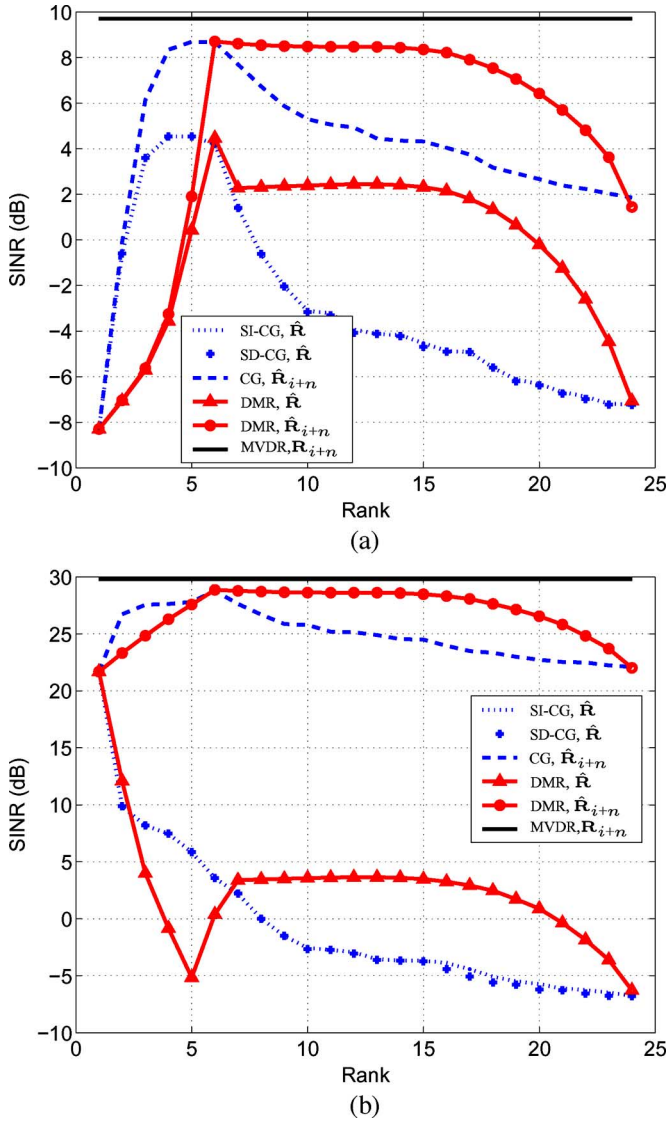

Fig. 1. SINR performance for the CG and DMR beamformer using $\hat{\mathbf{R}}$ and $\hat{\mathbf{R}}_{i+n}$ and 24 snapshots. (a) Low power signal at 0°. (b) High power signal at 7°.

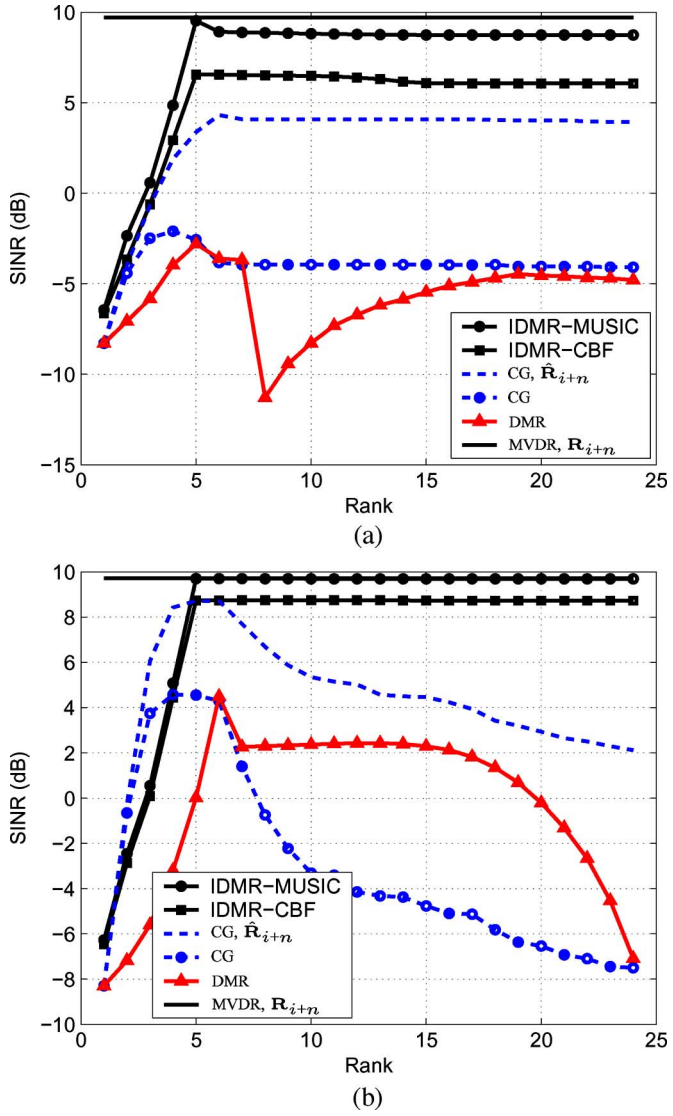

Fig. 2. SINR performance for low power signal at 0°. (a) Six snapshots. (b) Twenty-four snapshots.

own estimate. In accordance with Section IV, where we proved the equality of the SI-CG and SD-CG beamformers, the output SINR obtained with these two beamformers is shown to be the same. The MVDR beamformer with the true covariance matrix is plotted to serve as a reference of optimality.

In Fig. 1, we also show the case that the signal-free sample covariance matrix $\hat{\mathbf{R}}_{i+n}$ is available, and we plotted the output SINR employing the DMR and CG beamformers (from now on, we only refer to the CG beamformer, since SI-CG and SD-CG yield the same beamformer). The desired signal is not present in $\hat{\mathbf{R}}_{i+n}$. It can be observed that the output SINR is substantially higher when using $\hat{\mathbf{R}}_{i+n}$ than when using $\hat{\mathbf{R}}$. The degradation of the output SINR when using $\hat{\mathbf{R}}$ is not caused by the presence of the desired signal by itself, but by the effect of residual correlations between the desired signal and the interferers. We observe from (34) that the variance of the residual correlation is proportional to the power of the desired signal, to the power of the interferer, and to the inverse of the number of snapshots $(1/n)$. In Fig. 1(a), the desired signal (located at 0°) has a power of 20 dB (100 times) less than the desired signal (located at 7°) in Fig. 1(b). We observe that for the same number of 24 snapshots, the degradation when using $\hat{\mathbf{R}}$ instead of $\hat{\mathbf{R}}_{i+n}$ is much severe in the case of Fig. 1(b) (approximately 25 dB) than in the case of Fig. 1(a) (approximately 8 dB). This is because the variance of the residual correlations in Fig. 1(b) is 100 times larger than in Fig. 1(a).

Figs. 2 and 3 show the output SINR when the IDMR beamformer is used. The IDMR beamformer is implemented with both the CBF and MUSIC to locate the dominant peaks. While MUSIC yields finer estimates than the CBF, the former requires significantly more computational power. We observe that even when the CBF is used, the results are significantly better than those obtained using the existing low-rank beamforming techniques, such as CG and DMR. The reason for this improvement is that, in the IDMR technique, the residual correlations are not

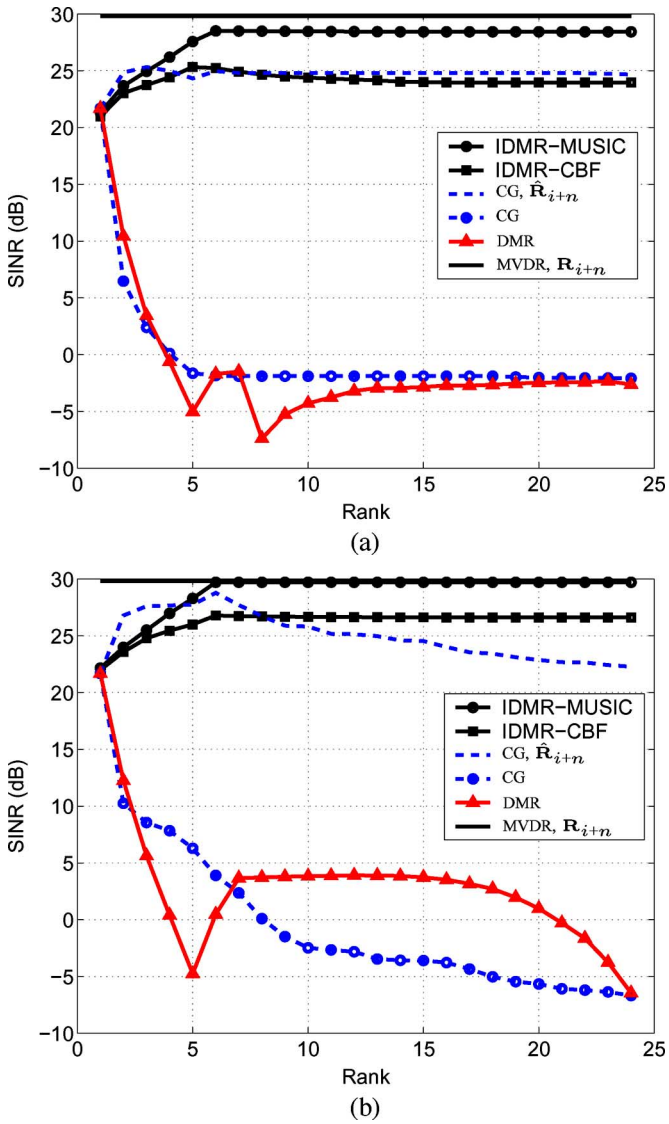

Fig. 3. SINR performance for low power signal at 7°. (a) Six snapshots. (b) Twenty-four snapshots.

present in the parametrically formed covariance matrix. It can be observed that the residual correlations is a big problem, especially under low sample support (see (34)). We observe in Figs. 2 and 3 that when the signal-free covariance matrix $\hat{\mathbf{R}}_{i+n}$ is used, the optimum SINR achieved using CG is close to the SINR obtained with the IDMR technique. Under higher sample supports, the effect of residual correlations is not so dramatic, and the improvement obtained with IDMR is not so expressive. The rank of the IDMR beamformer is the number of estimated signal directions used to form the matrix $\hat{\mathbf{A}}$. The directions are sorted by descending order of estimated signal power; that is, the steering vector of the signal with the strongest power is used as the first column of $\hat{\mathbf{A}}$ and so forth. The rank of the beamformer is equivalent to the number of columns of $\hat{\mathbf{A}}$. The number of spectrum peaks obtained with either MUSIC or the CBF is always smaller than $M = 24$, so the maximum rank of the IDMR beamformer is less than 24. The figures show the output SINR until the rank of 24. Thus, we repeat for the remaining ranks, the output SINR achieved when all the distinct peaks of the MUSIC or CBF spectrum have been incorporated into $\hat{\mathbf{A}}$. The IDMR beamformer requires an estimate of the noise power at the array elements; in the simulations, we used

$$\hat{\sigma}_n^2 = \lambda_{13} + \text{const} \tag{39}$$

where λ_{13} is the thirteenth-largest eigenvalue. We used $\sigma_n^2/1000$ as the constant; the purpose of this constant is to not let $\hat{\sigma}_n^2$ vanish when the number of snapshots is very small. When using MUSIC for a first estimate of the directions, we used only the 12 noise eigenvectors. In this particular case, a maximum of 18 could have been used, but we used only 12 for more conservative results. In addition to a higher output SINR than obtained with either CG and DMR, IDMR has the important advantage that the maximum SINR over all the ranks is very close to the SINR obtained at the maximum rank; thus, it is different from CG and DMR in that rank selection is not an issue (see Figs. 2 and 3).

Fig. 4 displays the plot of output SINR as a function of the number of snapshots. For the CG and DMR beamformers, the plotted SINR value is the average over 200 Monte Carlo simulation runs of the maximum SINR achieved over all possible ranks. For the IDMR beamformer, the plotted SINR value is the average of the SINR at the maximum rank. It is important to note that in a real-life situation, there is not a reliable way to select the optimal rank for the CG and DMR beamformers. Therefore, the curves show an upper-bound performance for the CG and DMR beamformers. We observe that the IDMR beamformer yields a high SINR even when a very small number of snapshots is used, e.g., with only five snapshots. When the number of snapshots is less than the number of array elements, the sample covariance matrix $\hat{\mathbf{R}}$ is singular, and a singular value decomposition (SVD) was used to estimate the noise subspace.

To illustrate the effect of residual correlations, Fig. 5 shows a plot of the output SINR as a function of rank for the case that the desired signal is truly correlated to an interferer. In this scenario, the desired signal (located at 0°) is partially correlated to the signal located at 7° with a correlation coefficient of $\rho = 0.5e^{j\pi/3}$. Twenty-four snapshots were used, in addition to the true correlation there is also the effect of the residual correlations due to the low sample support. We observe that even when the true covariance matrix is used to compute the MVDR beamformer, performance is still degraded. This is caused by the true correlation among signals. The IDMR beamformer cancels the correlation embedded in covariance matrix and the output SINR is significantly improved even when the CBF beamformer is used to estimate the directions of the dominant signals. Observe that when using the CG beamformer with the desired signal free sample covariance matrix $\hat{\mathbf{R}}_{i+n}$, the output SINR is similar to that obtained with the IDMR beamformer.

In Fig. 6, we compared the performance of the IDMR beamformer and the robust adaptive beamforming algorithm (RABA) proposed by Vorobyov *et al.* in [12]. RABA is known to be robust against low sample support and steering vector mismatch. To facilitate comparison, we used the same scenario which was

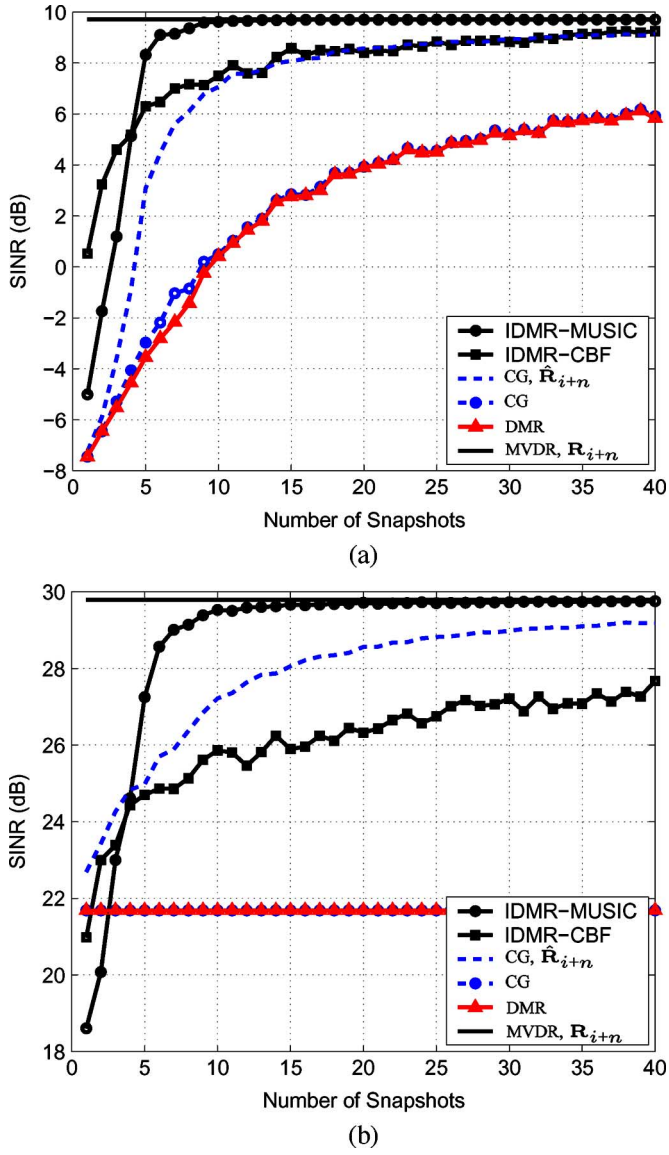

Fig. 4. Output SINR versus training sample size. (a) Signal at 0°. (b) Signal at 7°.

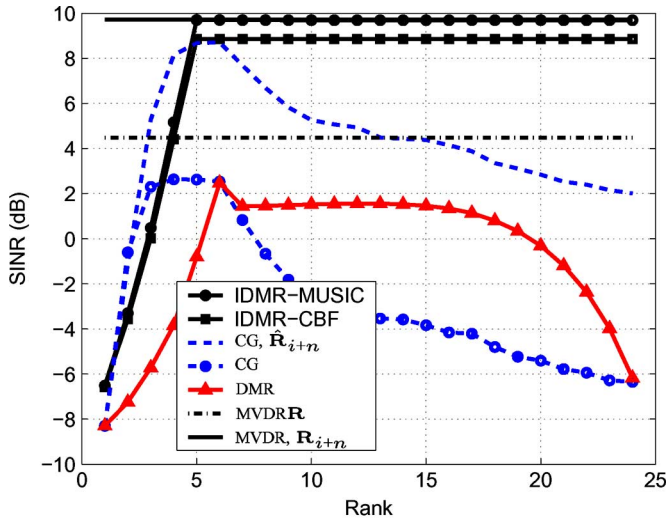

Fig. 5. Output SINR for truly correlated signals.

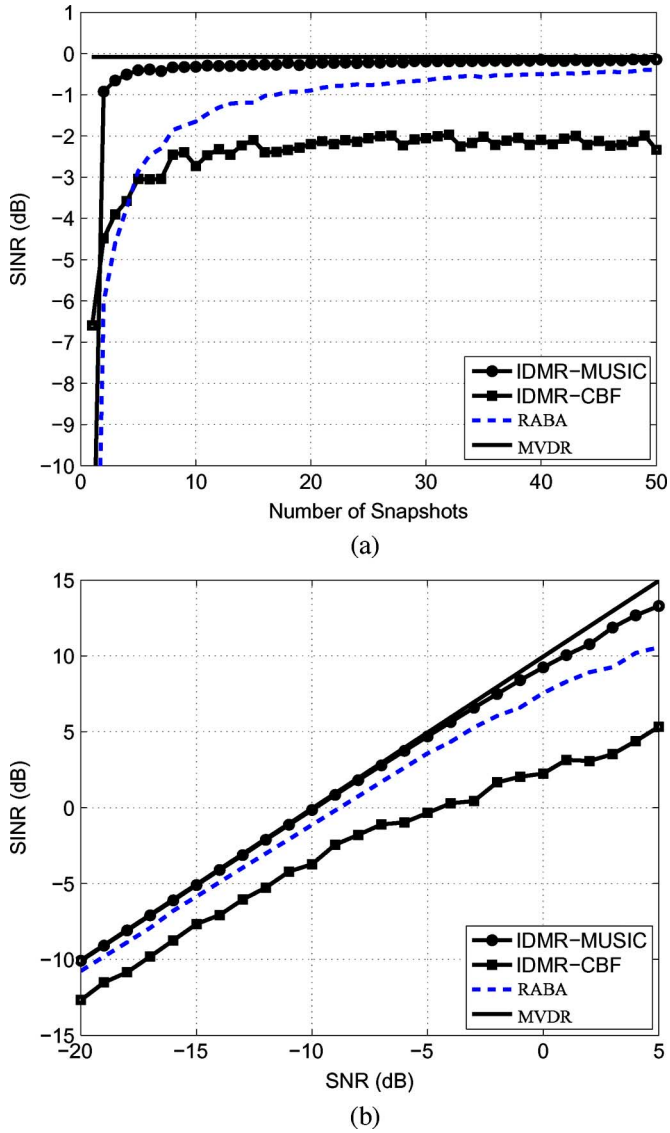

Fig. 6. Comparison with robust adaptive beamforming algorithm proposed by Varobyov *et al*. (a) Without look direction mismatch. (b) With look direction mismatch.

used in [12]. We considered the scenario with three uncorrelated signals arriving at the array with directions of arrival 3°, 30°, and 50° and SNRs of −10, 30, and 30 dB, respectively. The array is linear with ten omnidirecional sensors and half-wavelength spacing. The desired signal is the signal arriving at 3°. RABA was applied with the constant $\epsilon = 3$. In Fig. 6(a), there is no look-direction mismatch, and the output SINR is plotted versus the number of snapshots. In Fig. 6(b), there is a look-direction mismatch: the presumed and actual directions of arrival are 3° and 5°, respectively. In this simulation, 30 snapshots were used to estimate the sample covariance matrix, and the output SINR is plotted versus the SNR of the desired signal at 5°. When MUSIC is used in the first step of IDMR, the output SINR obtained with IDMR is shown to be higher than the obtained with RABA. In the case that the CBF is used in the first step of IDMR, then RABA yields a higher SINR.

VII. Conclusion

We analyzed existing low-rank beamformers and proved that SI-CG and SD-CG yield the same low-rank beamformer at any rank. This dictates the use of SI-CG in practice since it does not require the costly computation of blocking matrices. Under a situation of low sample support, we investigated the performance degradation of low-rank MVDR beamformers due to residual correlations embedded in the sample covariance matrix. This motivated us to propose a new adaptive beamforming technique (IDMR) based on a parametric estimate of the covariance matrix in which correlations among signals are effectively removed. Simulations revealed that the IDMR beamformer yields a dramatic improvement in the output SINR relative to existing CG and PCI/DMR beamformers, and unlike the CG and PCI/DMR beamformers the performance obtained with the IDMR beamformer does not depend on rank selection.

Appendix
Blocking Matrix Effected Through Householder Transformation

A Householder transformation is of the form

$$\mathbf{H} = \mathbf{I}_m - 2\mathbf{v}\mathbf{v}^H, \text{ where } \mathbf{v}^H\mathbf{v} = 1. \tag{40}$$

$\mathbf{I}_m$ is the $m \times m$ identity matrix. It can be shown that the matrix $\mathbf{H}$ is an unitary matrix for any unit norm vector $\mathbf{v}$. Without loss of generality, assuming that the steering vector $\mathbf{a}_1$ has a unit norm, we consider a unitary matrix constructed as

$$\mathbf{H} = [\mathbf{a}_1 \vdots \mathbf{B}] \tag{41}$$

where $\mathbf{B}$ is referred to as the blocking matrix, with $\mathbf{B}^H\mathbf{a}_1 = \mathbf{0}$ and $\mathbf{B}^H\mathbf{B} = \mathbf{I}_{m-1}$. It follows from these stipulations that $\mathbf{H}$ is a unitary matrix whose "action" on the steering vector is as follows:

$$\mathbf{H}^H\mathbf{a}_1 = \boldsymbol{\delta}_1 = \begin{bmatrix} 1 \\ 0 \\ \vdots \\ 0 \end{bmatrix}. \tag{42}$$

Substituting (40) into (42) implies that

$$\mathbf{v}\alpha\mathbf{a}_1 - \boldsymbol{\delta}_1 \tag{43}$$

where α indicates proportionality. Defining an $(m-1) \times m$ selection matrix, $\boldsymbol{\Gamma}$, as

$$\boldsymbol{\Gamma} = [\mathbf{0} \vdots \mathbf{I}_{m-1}] \tag{44}$$

we observe that

$$\mathbf{B}^H = \boldsymbol{\Gamma}\mathbf{H}^H. \tag{45}$$

Thus, through a Householder transformation, the blocking matrix $\mathbf{B}$ can be computed by

$$\mathbf{B} = (\mathbf{I}_m - 2\mathbf{v}\mathbf{v}^H)\boldsymbol{\Gamma}^T, \text{ where } \mathbf{v} = \frac{\mathbf{a}_1 - \boldsymbol{\delta}_1}{\|\mathbf{a}_1 - \boldsymbol{\delta}_1\|}. \tag{46}$$

Acknowledgment

The authors would like to thank the anonymous reviewers for their helpful comments and suggestions, which led to a better understanding of the IDMR beamformer and to a better organization of the paper.

References

[1] E. L. Santos and M. D. Zoltowski, "Adaptive beamforming with low sample support via indirect dominant mode rejection," in *Proc. IEEE Sensor Array Multichannel Signal Processing Workshop (SAM 2004)*, Barcelona, Spain, Jul. 2004, vol. S1–7, pp. 18–21.

[2] J. S. Goldstein, I. S. Reed, and L. L. Scharf, "Reduced rank adaptive filtering," *IEEE Trans. Signal Process.*, vol. 45, no. 2, pp. 492–496, Feb. 1997.

[3] M. Rangaswamy, F. C. Lin, and K. R. Gerlach, "Robust adaptive signal processing methods for heterogeneous radar clutter scenarios," *Signal Process.*, vol. 84, pp. 1653–1665, 2004.

[4] C. H. Gierull, "Statistical analysis of the eigenvector projection method for adaptive spatial filtering of interference," in *Proc. Inst. Elect. Eng. Sonar Navig.*, Huntsville, Apr. 1997, vol. 144, no. 2, pp. 57–63.

[5] G. N. Karystinos, H. Qian, M. J. Medley, and S. N. Batalama, "Short data record adaptive filtering: The auxiliary-vector algorithm," *Digit. Signal Process.*, vol. 12, pp. 193–222, Apr.–Jul. 2002.

[6] N. L. Owsley, "Data orthogonalization in sensor array processing," in *Proc. IEEE Sensor Array Multichannel Signal Processing Workshop (SAM 2002)*, Rosslyn, VA, Aug. 5–6, 2002, vol. 1, pp. 1–7.

[7] I. P. Kirsteins and D. W. Tufts, "Adaptive detection using low rank approximation to a data matrix," *IEEE Trans. Aerosp. Electron. Syst.*, vol. 30, no. 1, pp. 55–67, Jan. 1994.

[8] J. S. Goldstein, I. S. Reed, and L. L. Scharf, "A multistage representation of the Wiener filter based on orthogonal projections," *IEEE Trans. Inf. Theory*, vol. 44, no. 7, pp. 2943–2959, Nov. 1998.

[9] G. Dietl, M. D. Zoltowski, and M. Joham, "Reduced-rank equalization for EDGE via conjugate gradient implementation of multi-stage nested wiener filter," in *Proc. Vehicular Technology Conf. (VTC) 2001*, Oct. 2001, pp. 1912–1916.

[10] E. L. Santos and M. D. Zoltowski, "On low rank MVDR beamforming using the conjugate gradient algorithm," in *Proc. 2004 IEEE Int. Conf. Acoustics, Speech, Signal Processing*, Montreal, May 17–21, 2004, vol. 2, pp. 173–176.

[11] M. Rangaswamy, I. P. Kirsteins, B. E. Freburger, and D. W Tufts, "Signal detection in strong low rank compound-Gaussian interference," in *Proc. IEEE Sensor Array Multichannel Signal Processing Workshop*, Mar. 2000, pp. 144–148.

[12] S. A. Vorobyov, A. B. Gershman, and Z. Q. Luo, "Robust adaptive beamforming using worst-case performance optimization: A solution to the signal mismatch problem," *IEEE Trans. Signal Process.*, vol. 51, no. 2, pp. 313–324, Feb. 2003.

[13] X. Mestre and M. A. Lagunas, "Finite sample size effect on minimum variance beamformers: Optimum diagonal loading factor for large arrays," *IEEE Trans. Signal Process.*, vol. 54, no. 1, pp. 69–82, Jan. 2006.

[14] S. P. Applebaum and D. J. Chapman, "Adaptive arrays with main beam constraints," *IEEE Trans. Antennas Propag.*, vol. 24, no. 5, pp. 585–598, Sep. 1976.

[15] R. A. Monzingo and T. W. Miller, *Introduction to Adaptive Arrays*. New York: Wiley, 1980.

[16] E. K. P. Chong and S. H. Zak, *An Introduction to Optimization*. New York: Wiley, 2001.

[17] M. R. Hestenes and E. Stiefl, "Methods of conjugate gradients for solving linear systems," *J. Res. Natl. Bur. Stand.*, vol. 49, no. 6, pp. 409–436, Dec. 1952.

[18] L. N. Trefethen and D. Bau, III, *Numerical Linear Algebra*. Philadelphia, PA: SIAM, 1997.

[19] L. E. Brennan, J. D. Mallett, and I. S. Reed, "Adaptive arrays in airborne MTI radar," *IEEE Trans. Antennas Propag.*, vol. 24, no. 5, pp. 607–615, Sep. 1976.

[20] M. D. Zoltowski, "On the performance analysis of the MVDR beamformer in the presence of correlated interference," *IEEE Trans. Acoust., Speech, Signal Process.*, vol. 36, no. 6, pp. 945–947, Jun. 1988.

[21] R. O. Schmidt, "Multiple emitter location and signal parameter estimation," *IEEE Trans. Antennas Propag.*, vol. AP-34, no. 3, pp. 276–280, Mar. 1986.

Ernesto L. Santos was born in Brasília, Brazil, in 1972. He received the B.E. degree from the Federal University of Bahia, Brazil, in 1997, the M.S. degree from the State University of Campinas, Brazil, in 2000, and the Ph.D. degree from Purdue University, West Lafayette, IN, in 2005, respectively, all in electrical engineering.

He worked as a Research Assistant at Purdue University from 2003 to 2005. His research interests are in the area of signal processing and include adaptive beamforming and robust statistical signal processing.

Michael D. Zoltowski (S'79–M'86–SM'95–F'99) was born in Philadelphia, PA, on August 12, 1960. He received both the B.S. and M.S. degrees in electrical engineering with highest honors from Drexel University, Philadelphia, PA, in 1983 and the Ph.D. degree in systems engineering from the University of Pennsylvania, Philadelphia, in 1986.

In fall 1986, he joined the faculty of Purdue University, West Lafayette, IN, where he currently holds the position of Professor of electrical and computer engineering.

Dr. Zoltowski, in his capacity as Professor at Purdue, received the Ruth and Joel Spira Outstanding Teacher Award for 1990–1991 and the 2001–2002 Wilfred Hesselberth Award for Teaching Excellence, and in 2001, he was named a University Faculty Scholar. He was a corecipient of the IEEE Communications Society 2001 Leonard G. Abraham Prize Paper Award in the Field of Communications Systems. He was also the recipient of the IEEE Signal Processing Society's 1991 Paper Award The Fred Ellersick MILCOM Award for Best Paper in the Unclassified Technical Program at the 1998 IEEE Military Communications Conference, and a Best Paper Award at the 2000 IEEE International Symposium on Spread Spectrum Techniques and Applications. He is also the recipient of a 2002 Technical Achievement Award from the IEEE Signal Processing Society. In addition, he was selected as a 2003 Distinguished Lecturer for the IEEE Signal Processing Society. He was a recipient of the 2006 Distinguished Alumni Award from Drexel University. In addition, from 1998 to 2001, he was an elected Member-at-Large of the Board of Governors and Secretary of the IEEE Signal Processing Society. From 2003 to 2005, he served on the Awards Board of the IEEE Signal Processing Society and served as the Area Editor in charge of feature articles for the *IEEE Signal Processing Magazine*. Within the IEEE Signal Processing Society, he has been a member of the Technical Committee for the Statistical Signal and Array Processing Area, the Technical Committee for DSP Education and the Technical Committee on Signal Processing for Communications (SPCOM). From 2003 to 2004, he served as Vice-Chairman of the Technical Committee on Sensor and Multichannel (SAM) Processing and currently serves as Chairman. He has served as an Associate Editor for both the IEEE TRANSACTIONS ON SIGNAL PROCESSING and the IEEE COMMUNICATIONS LETTERS. He was Technical Co-Chairman of the 2006 IEEE Sensor Array and Multichannel Workshop.

Muralidhar Rangaswamy (S'89–M'93–SM'98–F'06) received the B.E. degree in electronics engineering from Bangalore University, Bangalore, India, in 1985 and the M.S. and Ph.D. degrees in electrical engineering from Syracuse University, Syracuse, NY, in 1992.

Previously, he has held industrial and academic appointments. He is presently employed as a Senior Electronics Engineer at the Sensors Directorate of the Air Force Research Laboratory (AFRL), Hanscom Air Force Base, MA. His research interests include radar signal processing, spectrum estimation, modeling non-Gaussian interference phenomena, and statistical communication theory. He has coauthored more than 70 refereed journal and conference record papers in the areas of his research interests. In addition, he is a contributor to three books and is a coinventor on two U.S. patents.

Dr. Rangaswamy is an Associate Editor for the IEEE TRANSACTIONS ON AEROSPACE AND ELECTRONIC SYSTEMS and is a member of the Sensor Array and Multichannel Processing Technical Committee (SAM-TC) of the IEEE Signal Processing Society. He was a coinstructor with Dr. W. Melvin for two short courses on space–time adaptive processing for the IEEE Boston section (April 2003) and for the IEEE Aerospace and Electronic Systems Society (AESS) Atlanta section at the Southeastern Symposium on System Theory (March 2004). He has served on the organizing committee of numerous IEEE AESS- and IEEE Signal Processing Society-sponsored conferences. He received the 2004 Fred Nathanson Memorial Radar Award from the IEEE AES Society, the 2006 Distinguished Member award from the IEEE Boston Section, and the 2005 Charles Ryan Basic Research Award from the Sensors Directorate of the Air Force Research Laboratory (AFRL), in addition to 20 AFRL scientific achievement awards.